

Supporting Information

Green Biosynthesis of Silver Nanoflowers Using *Tithonia diversifolia* Leaf Extract: In Vitro Anticancer Activity, Antimetastatic Effects, and Crystal Violet Photodegradation

Suganya Ganesan^{1,3}, Aswathy Karanath-Anilkumar^{2,3}, Jerome Rajendran^{4*} and Ganesh Munuswamy-Ramanujam^{1,3*}

¹ *Department of Chemistry, College of Science and Humanities, SRM Institute of Science & Technology, Kattankulathur, Chengalpattu 603203, India*

² *Department of Biotechnology, College of Engineering and Technology, SRM Institute of Science & Technology, Kattankulathur, Chengalpattu 603203, India*

³ *Interdisciplinary Institute of Indian System of Medicine, SRM Institute of Science & Technology, Kattankulathur, Chengalpattu 603203, India*

⁴ *Department of Electrical Engineering and Computer Science, University of California Irvine, CA, USA*

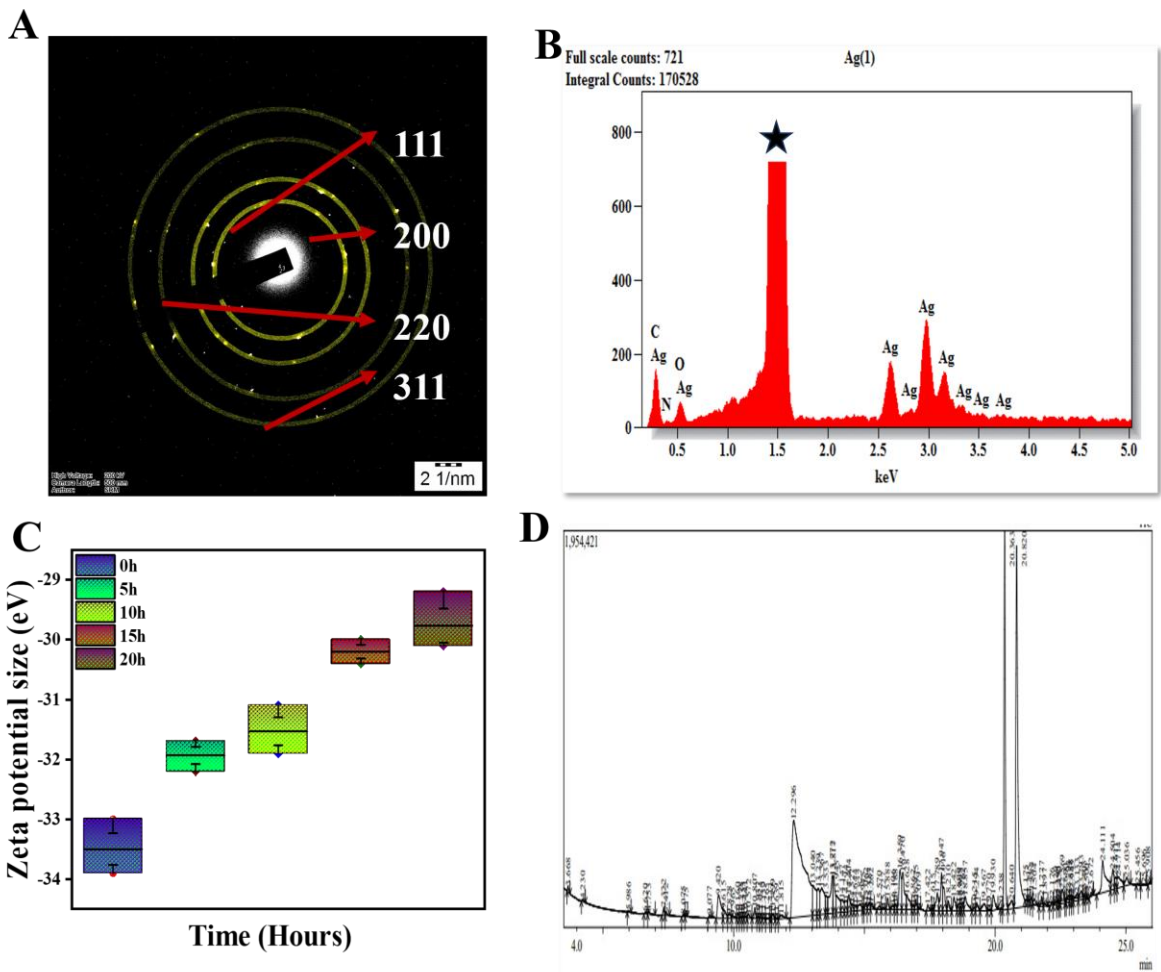
*Corresponding Authors

Jerome Rajendran, Email: jeromestil@gmail.com, rajendrj@uci.edu; ORCID: 0000-0001-8235-6382

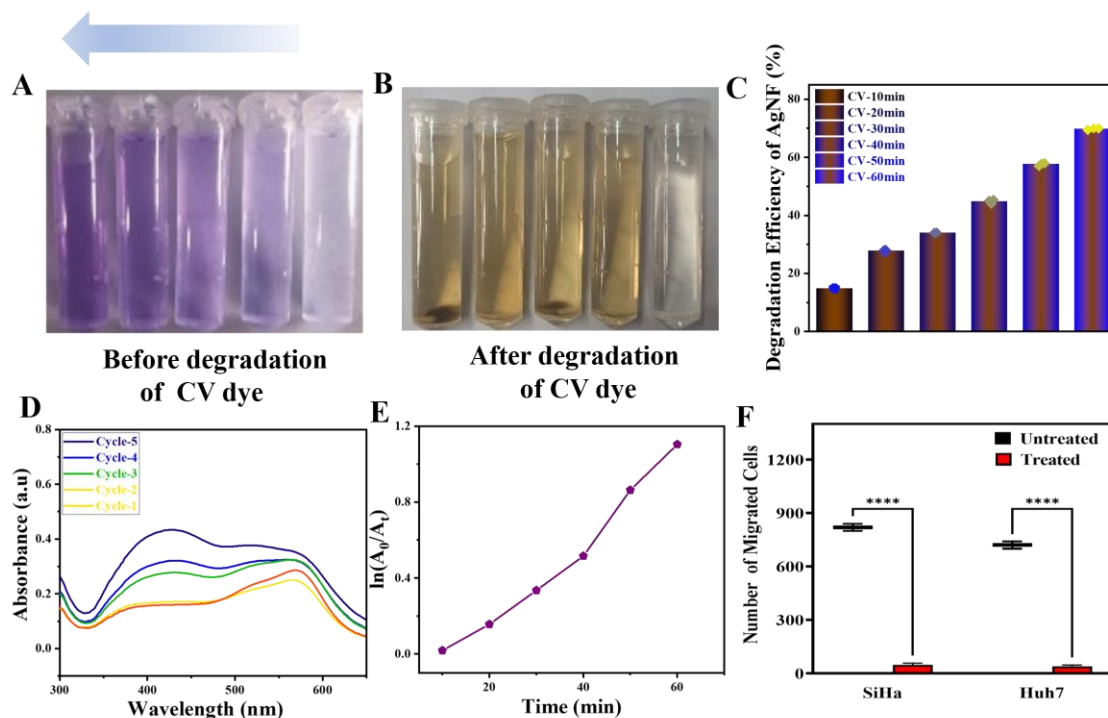
Ganesh Munuswamy Ramanujam, Email: mrganesh2000@hotmail.com, ganeshm1@srmist.edu.in; ORCID: 0000-0001-8021-601X



Supporting Fig. 1. Green synthesis of silver nanoflowers (AgNFs) using *Tithonia diversifolia* leaf extract (TDLE). (A) Preparation of plant precursor: *T. diversifolia* leaves were sun-dried and milled to a fine powder. (B) Synthesis scheme: the leaf powder was boiled in water for 10 min and filtered through Whatman paper to obtain TDLE; the extract was mixed with aqueous AgNO₃ for 30 min to reduce Ag⁺, producing a brown suspension; the product was collected by centrifugation and washing, then dried at 60 °C for 4 h to yield TD-AgNFs.



Supporting Fig. 2. Additional characterization of TD-AgNFs. (A) Selected area electron diffraction (SAED) pattern of TD-AgNFs, showing diffraction rings indexed to the crystalline Ag planes. (B) Energy-dispersive X-ray (EDX) spectrum of TD-AgNFs, confirming the elemental presence of silver. (C) Time-dependent zeta potential measurements of TD-AgNFs. (D) GC-MS chromatogram of *Tithonia diversifolia* leaf extract (TDLE).



Supporting Fig. 3. Additional evidence for crystal violet (CV) photocatalytic degradation and anti-migratory activity of TD-AgNFs. (A) Photographs of CV solutions before degradation, showing the characteristic violet color across increasing dye concentrations. (B) Corresponding images after TD-AgNF-mediated photocatalytic treatment, showing progressive decolorization. (C) Time-dependent CV degradation efficiency in the presence of TD-AgNFs (10–60 min). (D) UV–Vis absorbance spectra recorded over successive reuse cycles (Cycles 1–5) for evaluating TD-AgNF reusability. (E) Kinetic plot of CV degradation expressed as $\ln(A_0/A_t)$ versus irradiation time (0–60 min). (F) Quantification of Transwell migration in SiHa and Huh7 cells, showing reduced numbers of migrated cells in TD-AgNF-treated groups relative to untreated controls.

Table S1. Comparison of the present TD-AgNFs system with recently reported green-synthesized Ag-based nanoparticles/nanostructures.

No.	Nanoparticle / composition	Reported structure / morphology	Plant / green source used	Applications evaluated	Key performance / highlights	Ref
1	TD-AgNFs, present study	Hierarchical flower-like Ag nanoflowers; petal-like Ag plates; mesoporous structure	<i>Tithonia diversifolia</i> leaf extract	Anticancer, in vitro anti-migratory activity, antimicrobial/antifungal activity, antioxidant/ROS response, crystal violet decolorization	BET surface area 36.7 m² g⁻¹ ; IC ₅₀ values 0.16, 0.23, and 0.26 mg mL⁻¹ for Huh7, THP-1, and SiHa; migration inhibition at 50 μg mL ⁻¹ ; crystal violet decolorization; hierarchical AgNF platform; multi-application validation; BET-supported mesoporosity; biomedical–environmental integration	Present work
2	AgNFs	Flower-like Ag nanostructures	<i>Kalanchoe daigremontiana</i> leaf extract	Photocatalytic and antibacterial activity	Green-synthesized Ag nanoflowers showed enhanced antibacterial activity against <i>E. coli</i> and <i>S. aureus</i> and photocatalytic performance; limited biological scope; no anticancer/anti-migratory evaluation	¹
3	AgNPs	Ag nanoparticles	<i>Magnolia alba</i> leaf extract	Antimicrobial, antifungal, antiviral, anticancer, antioxidant, photocatalytic activity	Evaluated against multiple bacterial strains, <i>Candida albicans</i> , HCT-116 colon cancer cells, DPPH/FRAP-based antioxidant activity, and methyl orange dye photocatalysis; AgNP morphology; no nanoflower architecture; no migration assay	²
4	AgNPs	Irregular/rugged spherical nanoparticles	<i>Stachys tibetica</i> extract	Antioxidant, antimicrobial, photocatalytic activity	Rhodamine B degraded under sunlight within 1 h ; rate constant 0.066 min⁻¹ ; active against <i>Bacillus cereus</i> , <i>Pseudomonas</i> , <i>E. coli</i> , and <i>S. aureus</i> ; no anticancer evaluation; no anti-migratory study	³

5	AgNPs	Cluster-like/agglomerated; mostly spherical/oval particles, 16–22 nm by HR-TEM	<i>Momordica cymbalaria</i> leaf extract	Antioxidant, cytotoxicity, antibacterial, photocatalytic activity	DPPH inhibition 67.77% at 1000 $\mu\text{g mL}^{-1}$; IC_{50} 54.89 $\mu\text{g mL}^{-1}$ for MCF-7 and 160.74 $\mu\text{g mL}^{-1}$ for Vero cells; maximum antibacterial zone 17.33 mm against <i>E. coli</i> ; clustered AgNPs; no nanoflower/BET/migration correlation	4
6	Ag/AgCl NPs	Spherical and rod-shaped particles; ~20 and 75 nm	<i>Durio zibethinus</i> seed extract	Antibacterial, cytotoxicity, photocatalytic activity	SPR at 420 nm ; zeta potential -15.41 mV ; sunlight-assisted synthesis optimized at 4000 \pm 200 lux ; evaluated for methylene blue degradation; Ag/AgCl mixed phase; no anti-migratory validation	5
7	AgNPs	Spherical/oval nanoparticles; average size 28.32 nm	<i>Myrsine africana</i> leaf extract	Antibacterial, antioxidant, phytotoxic activity	UV-Vis peak at 438 nm ; highest antioxidant activity 57.7% at 40 $\mu\text{g mL}^{-1}$; DPPH IC_{50} 77.56 $\mu\text{g mL}^{-1}$; stronger antibacterial activity against <i>E. coli</i> ; phytotoxic focus; no anticancer/photocatalytic integration	6
8	Ag-TiO ₂ bimetallic NPs	Bimetallic nanoparticles; 10–60 nm	<i>Pluchea indica</i> leaf extract	Anticancer, antibacterial, antioxidant activity	IC_{50} 33.5 $\mu\text{g mL}^{-1}$ against MCF-7; IC_{50} 169.6 $\mu\text{g mL}^{-1}$ against Wi-38 normal cells; MIC 31.25–62.5 $\mu\text{g mL}^{-1}$; antioxidant IC_{50} 225 $\mu\text{g mL}^{-1}$, bimetallic system; no dye-degradation/migration study	7
9	AgNPs	Ag nanoparticles	<i>Cucumis prophetarum</i> aqueous leaf extract	Antibacterial and antiproliferative activity	Antibacterial and antiproliferative activity against cancer cell lines; limited application window; no photocatalytic or anti-migratory assessment	8

10	AgNPs	Ag nanoparticles	<i>Carissa carandas</i> leaf extract	Antioxidant and antibacterial activity	First report of <i>C. carandas</i> leaf-mediated AgNP synthesis for antioxidant and antibacterial activity; two-application scope; no anticancer/dye-degradation study	⁹
11	AgNPs	Ag nanoparticles	<i>Conocarpus lancifolius</i> fruit/plant extract	Antimicrobial and anticancer activity	Plant extract used to synthesize AgNPs for antimicrobial and anticancer evaluation against drug-resistant infection-related concerns; no nanoflower structure; no photocatalytic remediation	¹⁰
12	AgNPs	Small-sized AgNPs	<i>Viburnum grandiflorum</i> leaf extract	Antibacterial, antioxidant, anticancer activity	Biosynthesized AgNPs described as cost-effective and environmentally friendly, with antimicrobial and anticancer properties; no anti-migratory or dye-degradation validation	¹¹
13	AgNPs	Predominantly spherical; average diameter ~ 20 nm by TEM	<i>Brassica oleracea</i> leaf extract	Antibacterial, antioxidant, anticancer activity	Maximum antibacterial zones: 14.33 ± 0.57 mm against <i>S. epidermidis</i> and 12.0 ± 0.20 mm against <i>P. aeruginosa</i> ; MCF-7 IC ₅₀ 55 µg mL⁻¹ ; DPPH IC ₅₀ ~ 50.37 µg mL⁻¹ ; spherical AgNPs; no AgNF morphology; no environmental remediation	¹²
14	AgNPs	Ag nanoparticles	<i>Pandanus dubius</i> extract	Antioxidant, antibacterial, anticancer activity	UV–Vis absorption peak 458 nm ; FTIR identified functional groups involved in reduction/stabilization; limited mechanistic/functional integration; no anti-migratory or dye-degradation study	¹³
15	AgNPs	Ag nanoparticles	<i>Ammi visnaga</i> extract	Antibacterial, antibiofilm, anticancer,	99% inhibition against biofilm/bacteria; anticancer IC ₅₀ 17.1 ± 0.6 µg mL⁻¹ ; Eosin Y photodegradation	¹⁴

				Eosin Y photodegradation	up to 50% ; AgNP system; no nanoflower/BET-supported architecture; no migration assay	
16	AgNPs	Ag nanoparticles	<i>Aegle marmelos</i> leaf extract	Antimicrobial, antioxidant, anticancer, photocatalytic degradation	Integrated antimicrobial, antioxidant, anticancer, and photocatalytic degradation activity; conventional AgNPs; no hierarchical AgNF structure; no anti-migratory study	¹⁵
17	AgNPs	Ag nanoparticles	<i>Acer oblongifolium</i> plant extract	Antibacterial, antioxidant, antiproliferative activity	Reported IC ₅₀ values against MCF-7 and HeLa after 48–72 h, with values listed as 9.43 and 6.22 µg mL⁻¹ in the accessible text; antiproliferative focus; no photocatalytic/migration integration	¹⁶
18	AgNPs	Round AgNPs; 50–90 nm	<i>Lantana camara</i> leaf extract	Antibacterial and anticancer activity	IC ₅₀ 49.52 µg mL⁻¹ against A549 and 46.67 µg mL⁻¹ against MCF-7; round AgNPs; antibacterial–anticancer only; no dye-degradation study	¹⁷
19	AgNPs	Ag nanoparticles	<i>Justicia brandegeana</i> aqueous extract	Antibacterial, antioxidant, anticancer activity	Reported as a green-synthesized AgNP system for combined antibacterial, antioxidant, and anticancer evaluation; no nanoflower morphology; no anti-migratory/photocatalytic validation	¹⁸
20	AgNPs	Ag nanoparticles	<i>Odontosoria chinensis</i> leaves	Antibacterial, antioxidant, anticancer activity	Synergistic antibacterial effects, antioxidant potential, and anticancer activity; AgNP structure; no environmental remediation or migration assay	¹⁹
21	AgNPs	Ag nanoparticles; 50–110 nm , average ~70 nm	<i>Elaeocarpus serratus</i> / Ceylon olive extract	Antibacterial activity	AgNPs in the 50–110 nm range; proteins, phenols, and flavonoids involved in reduction/capping;	²⁰

					antibacterial-only scope; no multifunctional biological–environmental testing	
22	AgNPs	Ag nanoparticles	<i>Melaleuca alternifolia</i> leaf extract	Antibacterial, antifungal, antioxidant, anticancer activity	Tea-tree-leaf-mediated AgNPs with antibacterial, antifungal, antioxidant, and anticancer activities; no photocatalytic dye decolorization; no anti-migratory assessment	²¹
23	AgNPs	Ag nanoparticles	<i>Barleria gibsonii</i> extract	Antibacterial, antioxidant, cytotoxic, catalytic activity	<i>B. gibsonii</i> -AgNPs with antibacterial, antioxidant, cytotoxic, and catalytic activities; conventional AgNPs; no AgNF morphology; no CV decolorization/migration integration	²²
24	Ag ₂ O NPs	Silver oxide nanoparticles	<i>Eruca sativa</i> extract	Biological activities	<i>E. sativa</i> -mediated Ag ₂ O nanoparticles with biological activity; silver oxide phase; no metallic AgNF architecture; no biomedical–photocatalytic integration	²³
25	AgNPs	Ag nanoparticles	<i>Alcea rosea</i> leaf aqueous extract	Biological activities	<i>Alcea rosea</i> -mediated AgNPs with biological activity; conventional AgNPs; no AgNF morphology; no BET/migration/CV-decolorization study	²⁴

Table S2. Structural parameters calculated from XRD peaks of TD-AgNFs

Plane (hkl)	2 theta (deg)	FWHM (2theta)	FWHM (rad)	d-spacing (Å)	Crystalline size (nm)	Lattice parameter (Å)	Micro strain (ϵ)	Dislocation density (m^{-2})
(111)	37.98	0.6927	0.01209	2.3835	12.1	4.10	8.86×10^{-3}	6.83×10^{15}
(200)	44.17	0.5196	0.00907	2.0482	16.8	4.09	5.6×10^{-3}	3.5×10^{15}
(220)	64.35	0.5196	0.00907	1.4477	18.7	4.08	3.5×10^{-3}	2.9×10^{15}
(311)	77.32	0.5196	0.00907	1.2346	20.4	4.11	2.8×10^{-3}	2.4×10^{15}

Supporting Reference

- 1 G. A. Molina, R. Esparza, J. L. López-Miranda, A. R. Hernández-Martínez, B. L. España-Sánchez, E. A. Elizalde-Peña and M. Estevez, *Colloids Surf. B. Biointerfaces*, 2019, **180**, 141–149.
- 2 S. De Mel, J. Gruenler, L. Khoury, A. Heynes, J. Fazekas, K. Damaske, T. Galbadage, R. S. Gunasekera and R. S. Anderson, *Sci. Rep.*, 2025, **15**, 23709.
- 3 N. A. Dar, P. A. Dar, M. Qadir and W. A. Shah, *Sci. Rep.*, 2025, **15**, 29673.
- 4 M. Sundar, G. Rajagopal, A. Nivetha, S. Prabu Kumar and S. Muthukumar, 2024, DOI: 10.3390/separations11020061.
- 5 S. Sumitha, S. Vasanthi, S. Shalini, S. V Chinni, S. C. B. Gopinath, P. Anbu, M. B. Bahari, R. Harish, S. Kathiresan and V. Ravichandran, 2018, DOI: 10.3390/molecules23123311.
- 6 Q. Sarwer, M. S. Amjad, A. Mehmood, Z. Binish, G. Mustafa, A. Farooq, M. F. Qaseem, F. Abasi and J. M. Pérez de la Lastra, 2022, DOI: 10.3390/molecules27217612.
- 7 S. Selim, B. M. Badr, M. H. Moustafa, E. Saied, F. M. Elkady, A. salama, A. S. Aloufi, N. A. Algamdi, N. N. Alzahofi, E. Abada, M. S. Alshammari, S. K. Al Jaouni and A. H. Hashem, *Sci. Rep.*, 2025, **15**, 26735.
- 8 Hemlata, P. R. Meena, A. P. Singh and K. K. Tejavath, *ACS Omega*, 2020, **5**, 5520–5528.
- 9 R. Singh, C. Hano, G. Nath and B. Sharma, 2021, DOI: 10.3390/biom11020299.
- 10 M. Oves, M. Ahmar Rauf, M. Aslam, H. A. Qari, H. Sonbol, I. Ahmad, G. Sarwar Zaman and M. Saeed, *Saudi J. Biol. Sci.*, 2022, **29**, 460–471.
- 11 H. Talib, A. Mehmood, M. S. Amjad, A. Mustafa, M. A. R. Khan, M. Raffi, R. T. Khan, K. S. Ahmad and H. Qureshi, *Bot. Stud.*, 2024, **65**, 4.
- 12 S. Ansar, H. Tabassum, N. S. M. Aladwan, M. Naiman Ali, B. Almaarik, S. AlMahrouqi, M. Abudawood, N. Banu and R. Alsubki, *Sci. Rep.*, 2020, **10**, 18564.
- 13 S. Velmani, E. N. Sholkamy, P. Ruba, S. Kanaga, V. Balamurugan, M. A. Tarighat and G. Abdi, *Sci. Rep.*, 2025, **15**, 39940.
- 14 U. Farooq, A. K. Qureshi, H. Noor, M. Farhan, M. E. Khan, O. A. Hamed, A. H. Bashiri and W. Zakri, 2023, DOI: 10.3390/plants12122337.
- 15 P. Rama, P. Mariselvi, R. Sundaram and K. Muthu, *Heliyon*, DOI:10.1016/j.heliyon.2023.e16277.
- 16 M. Naveed, B. Bukhari, T. Aziz, S. Zaib, M. A. Mansoor, A. A. Khan, M. Shahzad, A. S. Dabool, M. W. Alruways, A. A. Almalki, A. S. Alamri and M. Alhomrani, *Molecules*, DOI:10.3390/molecules27134226.
- 17 L. V Hublikar, S. V Ganachari, V. B. Patil, S. Nandi and A. Honnad, *Prog. Biomater.*, DOI:10.1007/s40204-023-00219-9.

- 18 N. M. Alassadi, G. J. Al-Ghizzawi, A. M. Amshawee and R. Ali, *Next Nanotechnol.*, 2025, **8**, 100275.
- 19 S. Ghosh and S. N. Sinha, *Next Nanotechnol.*, 2025, **8**, 100316.
- 20 K. M. Fernando, C. A. Gunathilake, C. Yalagama, U. K. Samarakoon, C. A. N. Fernando, G. Weerasinghe, G. K. Pamunuwa, I. Soliman, N. Ghulamullah, S. M. Rajapaksha and O. Fatani, 2024, DOI: 10.3390/jcs8020043.
- 21 B. M. Dayana, R. Venkatesan, J. T. Joseph Prakash, P. Saravanan, M. S. Nivetha, A. Murali, A. A. Vetcher, M. Settu and S.-C. Kim, *Sci. Rep.*, 2026, **16**, 2574.
- 22 S. S. M. Ali, K. Dharmadhikari, K. I. Saiyed, H. Vasava, M. A. Jowhari and P. Robin, *Sci. Rep.*, 2026, **16**, 8281.
- 23 F. Gul, Z. Ullah, J. Iqbal, B. A. Abbasi, S. Ali, S. Kanwal, J. Uddin, M. Kazi and T. Mahmood, *Sci. Rep.*, 2025, **15**, 13466.
- 24 I. Ojha, P. S. Saud, D. R. Jaishi, Y. R. Rosyara, A. Ojha, N. R. Devi, P. R. Joshi and H. R. Pant, *Sci. Rep.*, 2026, **16**, 6693.